Available online at www.sciencedirect.com
ScienceDirect
Surface & Coatings Technology 201 (2007) 6285–6289
SURFACE & COATINGS TECHNOLOGY
www.elsevier.com/locate/surfcoat

Formation of nanoporous titania on bulk titanium by hybrid surface mechanical attrition treatment

Ming Wen [a,b,*], Jian-Feng Gu [a], Gang Liu [b], Zhen-Bo Wang [b], Jian Lu [c]

[a] School of Materials Science and Engineering, Shanghai Jiao Tong University, Shanghai, 200030, PR China
[b] Shenyang National Laboratory for Materials Science, Institute of Metals Research, Chinese Academy of Sciences, Shenyang, Niaoning, 110016, PR China
[c] Mechanical Engineering Department, The Hong Kong Polytechnic University, Hong Kong, PR China

Received 1 November 2006; accepted in revised form 23 November 2006
Available online 22 January 2007

Abstract

Titanium has been used as an important implant material in humans, and it is important to investigate the interaction between titanium and H_2O_2 produced from the inflammatory response during the implantation procedure. However, the reports about the interaction between H_2O_2 and nanostructured or ultrafine-grained Ti are still very limited. In this work, the interaction between H_2O_2 and bulk Ti with a nanostructure surface was reported. At first, a commercial pure Ti plate underwent a surface mechanical attrition treatment (SMAT) in vacuum for 1 h to produce a nanocrystalline layer of Ti about 30 μm thick. Then the SMAT Ti was immersed into hydrogen peroxide solution for 24 h at 25 °C, and nanoporous titania was produced on the SMAT Ti surface. The nanoporous structure could be retained even after calcinations at 600 °C, while only intergranular corrosion appeared in coarse-grained Ti after the same chemical treatment.

PACS: 61.46.HK; 68.35.BS
Keywords: Nanocrystalline; Nanoporous; Titania; SMAT

1. Introduction

Titanium has been used as an important implant material in humans, especially in load-bearing and orthopedic implant applications [1–3]. The insertion of an implant is inevitably associated with an inflammatory response due to the surgical trauma, and during which superoxide radicals and H_2O_2 are formed at the site of surgery if the degradation products are improper, so it is important to investigate the interaction between titanium surface and H_2O_2. Tengvall et al. had extensively investigated the interaction of Ti power and H_2O_2 in 1989 [4–6]. Recently, Osaka et al. oxidized commercial pure Ti plate by H_2O_2 at 80 °C for 1 h, and they got submicrometer-sized porous titania on the surface of Ti, which showed good biocompatibility after further calcinations [7,8]. When the oxidation time extended to 72 h, well-aligned nanorods appeared on the surface which detached readily after ultrasonically cleaning [9], and the photocatalytic activity was also very good [10]. But when the temperature fell to room temperature (25 °C), Ti plate showed intergranular corrosion after 24 h in the same solution [11].

Due to unusual high strength, physical and mechanical properties that nanostructured and ultrafine-grained materials possess, extensive research has been done during the past years, especially bulk ultrafine-grained Ti made by severe plastic deformation (SPD) with the aim of using them as bone implant and high strength thread in the human body [12,13]. But until now, research on the interaction between H_2O_2 and nanostructured or ultrafine-grained Ti is still very limited. The newly developed surface mechanical attrition treatment is an effective way to realize surface self-nanocrystallization on metallic materials without changing the chemical compositions. The key point of SMAT is to introduce a large amount of defects and/or interfaces into the surface layer by repeated multidirectional impacts at high strain rate over a short period of time, so the microstructure of entire sample surface is transformed from coarse grain into nanometer scale progressively [14,15].

* Corresponding author. School of Materials Science and Engineering, Shanghai Jiao Tong University, Shanghai, 200030, PR China. Tel.: +86 21 34203743; fax: +86 21 34203742.
E-mail address: wenming127@sjtu.edu.cn (M. Wen).

0257-8972/$ - see front matter © 2006 Elsevier B.V. All rights reserved.
doi:10.1016/j.surfcoat.2006.11.031

Previous investigation showed that a nanostructured surface layer up to 30 μm could be achieved on commercial pure Ti by SMAT [16]. Herein, we report the products from the interaction of H_2O_2 and bulk Ti with a nanostructure surface at room temperature, and the influence of the following calcination on the structure changes of the treated surface.

2. Experimental

The material used in this study was a commercial pure Ti plate ($110 \times 40 \times 2$ mm^3) with the chemical composition (wt.%): 0.10 Fe, 0.01 Si, 0.16 O, 0.014 N, 0.004 H, 0.022 C and 0.23 Al. The plate was annealed in argon atmosphere at 740 °C for 2 h, and then air-cooled, resulting in equiaxed grains averaging 30 μm in size. The SMAT set-up had been described in detail elsewhere [14,15]. In this study, the vibration frequency of the system was 50 Hz; stainless steel balls with the diameter of 8 mm were used and the samples were treated in vacuum for 60 min at room temperature.

The SMAT Ti plate was cut into squares with the size of $10 \times 10 \times 2$ mm^3 by using electro-discharging. After pickling with 1 M HCl for 1 min and ultrasonic washing with acetone, absolute alcohol, and distilled water for 15 min, the SMAT Ti plate was immersed into 30 wt.% H_2O_2 for 24 h at room temperature. After that, the plate was rinsed with distilled water and dried at 40 °C for 6 h. Finally, the as-dried plate was calcinated at elevated temperature in air for 1 h. For comparison, a coarse-grained Ti was also prepared according to the same procedure only in the absence of SMAT, and the pickling procedure was just the same as in [7]. The phase constitutions of the as-prepared sample's surface were characterized by the Raman spectra (Jobin Yvon HR800, 632.8 nm laser). Scanning electron microscopy analyses (SEM: Supra 35 LEΦ FSEM and XL 30 ESEM) were conducted to examine the surface morphologies of the as-prepared samples. Transmission electron microscopy (TEM: JEOL-2010) observations with an accelerating voltage of 200 kV were then used to characterize the titania on the SMAT sample surface. The titania was removed from the sample surface by scraping it carefully into a bottle with absolute alcohol, and then collected by a carbon-coated copper grid for TEM analyses.

3. Results and discussion

Fig. 1 shows the Raman spectra of both coarse-grained Ti and SMAT Ti. There is no band in the Raman spectra of three states of coarse-grained samples (Fig. 1a): without oxidation, with oxidation, with oxidation and calcination at 400 °C; but two sharp bands at 448, 612 cm^{-1} and a broad band at 243 cm^{-1} are presented in the coarse-grained sample after oxidation and calcination at 600 °C, which can respectively be assigned to the Raman active fundamental mode of E_g, A_{1g}, and the second-order scattering or disorder of rutile [17]. Fig. 1b shows the great difference in the Raman spectra of the SMAT samples. Although there is also no band in the sample without oxidation, a weak band at 156 cm^{-1} appears in the sample with oxidation. Calcined further at 400 °C, the band at 156 cm^{-1} moves to

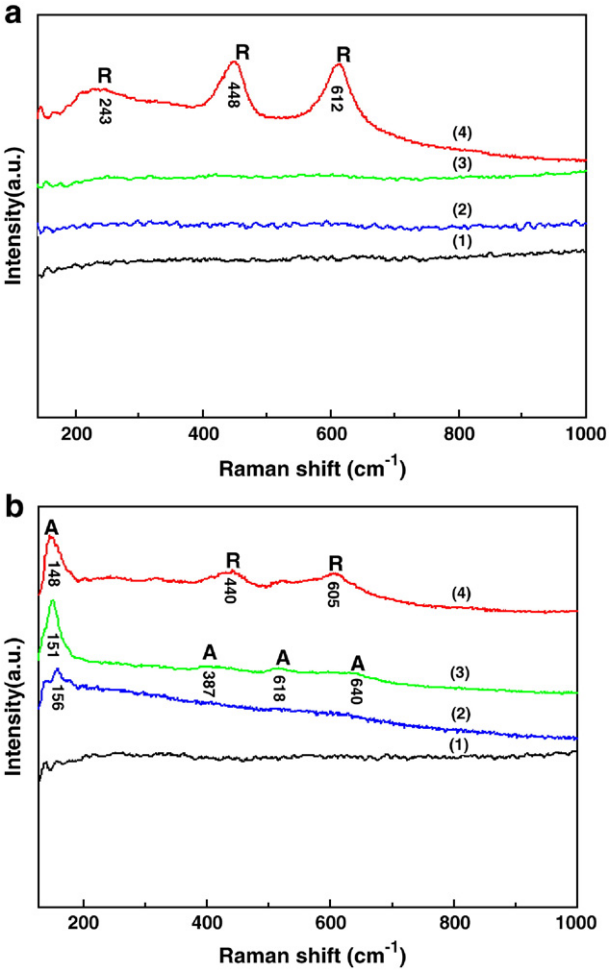

Fig. 1. Raman spectra of coarse-grained Ti (a) and SMAT Ti (b). (1): Before oxidation; (2): oxidation at room temperature for 24 h; (3): post-calcination of (2) at 400 °C for 1 h; (4): post-calcination of (2) at 600 °C for 1 h. The bands labelled R and A are rutile and anatase, respectively.

151 cm^{-1} and becomes much more intense and sharp, and three broad bands at 397, 518 and 640 cm^{-1} are also presented; these four bands correspond well to E_g, B_{1g}, $A_{1g}+B_{1g}$ and E_g of anatase respectively [17]. When raising the calcination temperature to 600 °C, it is clear that the surface is a mixture of anatase and rutile (148 cm^{-1}: E_g of anatase; 440 and 605 cm^{-1}: E_g and A_{1g} of rutile, respectively).

Fig. 2 shows the SEM images of coarse-grained Ti and SMAT Ti after oxidation and calcination. After oxidation for 24 h in H_2O_2, intergranular corrosion appeared in the coarse-grained sample (Fig. 2a), just the same as in [11], which is caused by the higher chemical reactivity of grain boundary than that of the grain interior. It also has no obvious change after further calcination at 400 °C (Fig. 2b), while numerous oxide nucleii and some stacks of bigger oxide granules (see insert in Fig. 2c) appear after calcination at 600 °C suggesting that nonhomogeneous oxidation behavior came into being. In the SMAT sample, the surface is almost composed of flakes and cones after oxidation for 24 h, and higher magnification inserted shows that the flakes and cones are besprinkled with very small holes in the nanometer scale (Fig. 2d). With further calcination

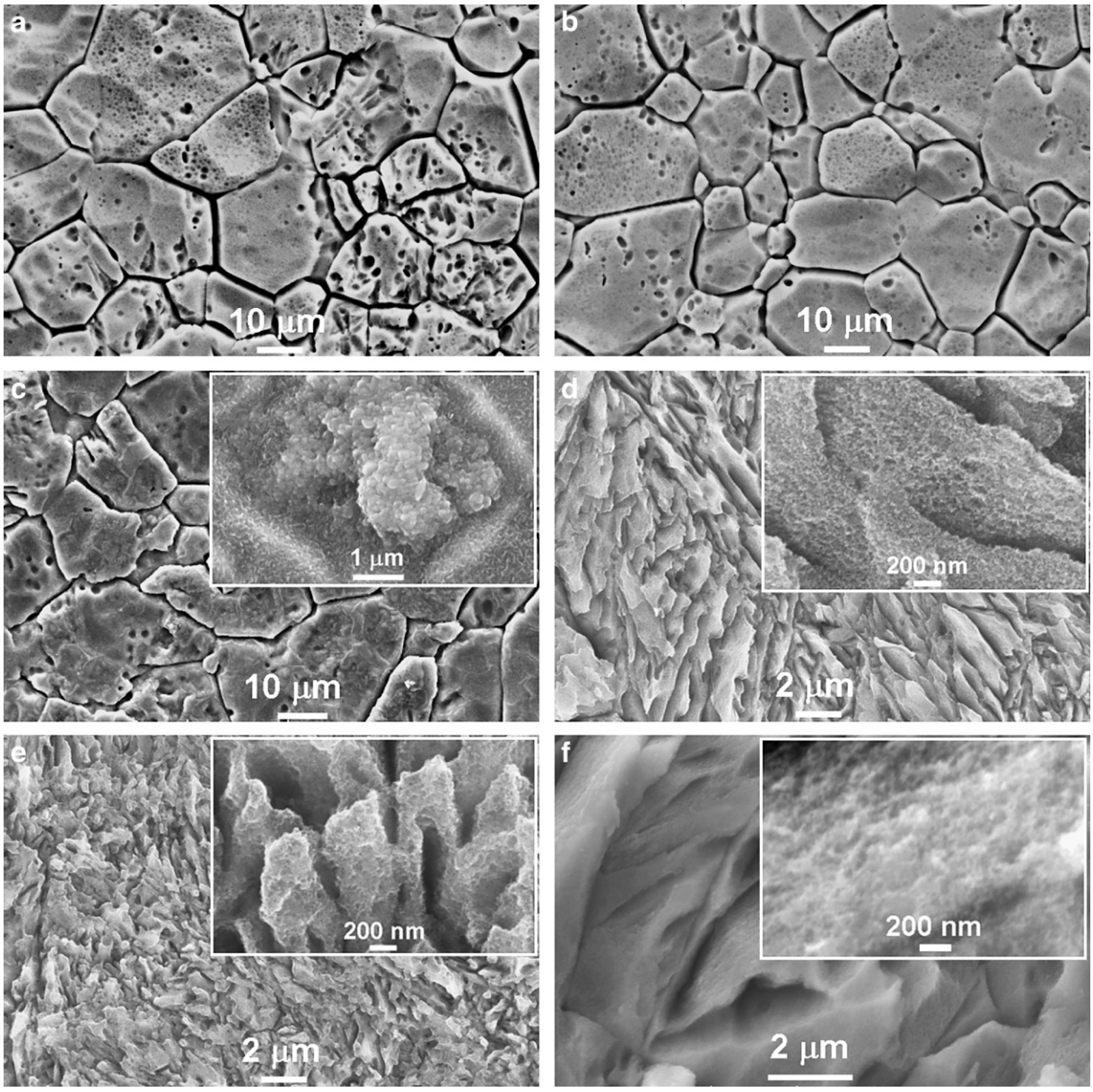

Fig. 2. SEM pictures of coarse-grained Ti (a–c) and SMAT Ti (d–f) top surface. (a): Coarse-grained Ti after oxidation at room temperature for 24 h; (b): post-calcination of (a) at 400 °C for 1 h; (c): post-calcination of (a) at 600 °C for 1 h; (d): SMAT Ti after oxidation at room temperature for 24 h; (e): post-calcination of (d) at 400 °C for 1 h; (f): post-calcination of (d) at 600 °C for 1 h.

at 400 °C, numerous randomly oriented coral reefs are presented and each coral is also full of nanometer-sized holes (Fig. 2e). Raising the calcination temperature to 600 °C, though the coral becomes coarser due to the coalescence of titania at higher temperatures, the surface full of nanometer-sized holes can still be retained (Fig. 2f).

TEM images of the SMAT Ti surface (before oxidation) are presented in Fig. 3a,b. Both bright field and dark field images show that the grains are mostly equiaxed and high dislocation densities exist both in some grains and the grain boundaries. A nanocrystalline layer of Ti about 30 μm thick was formed after SMAT, in which the average grain size was about 103 nm measured from a number of TEM images. Below the nanocrystalline layer, the grain size increased from nanometer to micrometer gradually. The TEM pictures of SMAT treated Ti calcined at elevated temperature are shown in Fig. 3c,d. A clear nanoporous structure is presented in the sample calcined at 400 °C (Fig. 3c), and the pore size varies from 10 to 30 nm which agrees very well with the SEM observations (Fig. 2e). The corresponding Energy dispersive spectroscopy (EDS) analysis (Fig. 3d) demonstrates no contaminations exist in our sample (Note: the Cu peaks at 8.045, 8.892 keV belong to the Cu grid supporting the sample.) The SAED pattern shows ambiguous rings, which means that the crystallinity in this sample is relatively poor. It is evident that the nanoporous structure can also be retained in the sample calcined at 600 °C (Fig. 3e), and the shape of the rings in the SAED pattern is more distinct, indicating an improvement of the crystallinity.

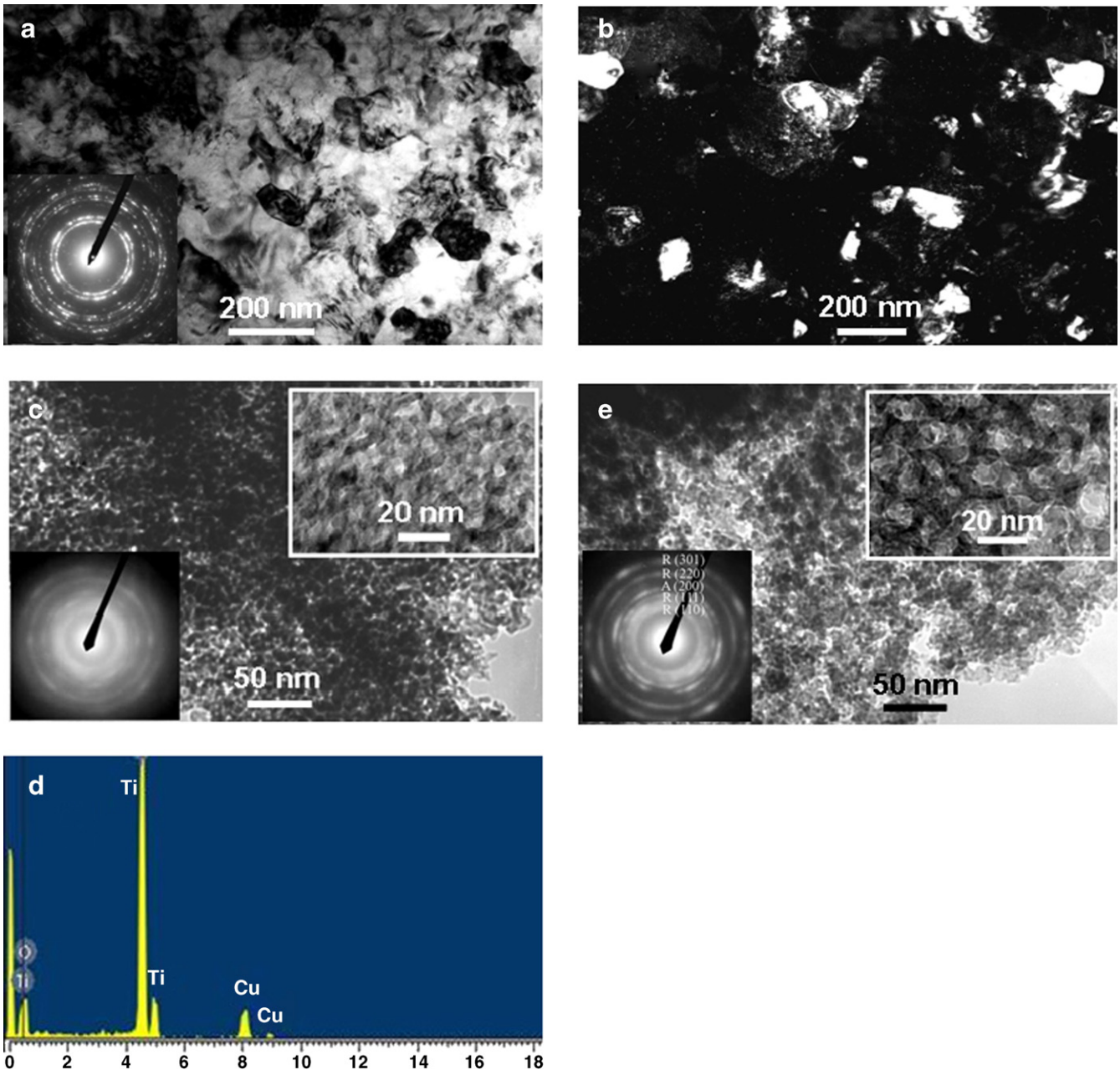

Fig. 3. (a) and (b): Bright field image and dark-field image of nanocrystalline Ti at about 15 μm below top surface of SMAT Ti (before oxidation); (c): bright field image of SMAT Ti top surface with oxidation at room temperature for 24 h and calcination at 400 °C for 1 h; (d): the corresponding EDS of (c); (e): bright field image of SMAT Ti top surface with oxidation at room temperature for 24 h and calcination at 600 °C for 1 h. R and A in SAED are rutile and anatase, respectively.

The reactions between the titanium substrate and H_2O_2 can be interpreted by considering that the oxidation of titanium, titania gel formation and Ti (IV) dissolution occurred competitively though the oxidation mechanism is still not clarified [18]. Tengvall et al. suggested that H_2O_2 occurring during a respiratory burst forms a TiOOH matrix, at least as an intermediate form, on and outside a TiO_2 layer; the matrix formation may also be the cause of the growth of oxide layer in vivo [5,6]. The nanoporous titania formation mechanism during the immersion of SMAT Ti into H_2O_2 solution is still not understood and needs more intense investigations. It should be noted that Raman spectroscopy is very sensitive to titania crystalline because of the enhanced scattering associated with crystalline boundaries. Wu et al. found no Raman bands at 144 cm^{-1} which corresponds to the strongest band of anatase after oxidizing coarse-grained Ti plate in H_2O_2 at 80 °C for 72 h and further calcination at 450 °C for 1 h, and they attributed that to oxygen deficiency [9,10]. But when we oxidized SMAT Ti in the same solution as Wu at 25 °C, a weak band at 156 cm^{-1} appeared and the band shift can be attributed to the small grain size and oxygen deficiencies [19]. Since it is well known that amorphous titania has no Raman bands [9], then it can be confirmed that crystalline anatase was produced. One possible route to obtain the crystalline titania

under the present soft solution condition is the *in situ* crystallization of the amorphous titania gel. Ooka et al. also found that TiO_2 nanoparticle in the pillared montmorillonite was crystallized to anatase phase by treatment with aqueous hydrogen peroxide at room temperature without losing both the porous structure and the hydrophobicity of the pillared clay [20]. At the same time, the nitriding and chromizing behavior of iron and low carbon steel has been systematically studied in [21–24], and the authors found that the treatment temperature of SMAT sample is much lower than that of the coarse-grained counterparts. The high chemical reactivity of the nanocrystalline and a large excess energy in the form of non-equilibrium defects bring an extra driving force stored on the SMAT Ti surface, which makes it possible for the amorphous titania formed in H_2O_2 solution to change into titania with weak crystallinity. At the same time, the aqueous environment improved the diffusivity of atoms remarkably, which also helped the nucleation and growth of crystalline phases [7]. The crystallinity is much improved after further calcination at 400 °C for 1 h, while the coarse-grained Ti showed no change after the same process.

4. Conclusions

In conclusion, the hybrid SMAT method produces nanoporous titania on bulk Ti by *in situ* synthesis without introducing external media (such as template, sputtering or sol–gel method). The Raman spectra confirm that crystalline titania formed on the SMAT Ti surface during immersion in the H_2O_2 solution, and the following calcination shows that the nanoporous structure can be retained even after calcinations at 600 °C suggesting high thermal stability. The nanoporous structure formation mechanism is still unknown. It is a novel and simple technique of preparing nanoporous titania, though it needs further optimization and explanation.

Acknowledgements

This work was supported by NSFC (Grant No. 50431010), Most of China (Grant No. 2005CB623604) and the Hong Kong Polytechnic University (Grant No. BB90). We thank Dr. Li-Hua Qian and Dr. Yan-Bo Wang for helpful discussions and their insights.

References

[1] T. Kokubo, H.M. Kim, M. Kawashita, T. Nakamura, J. Mater. Sci., Mater. Med. 15 (2004) 99.
[2] X.Y. Liu, P.K. Chu, C.X. Ding, Mater. Sci. Eng., R 47 (2004) 49.
[3] S. Nishiguchi, H. Kato, M. Neo, M. Oka, H.M. Kim, T. Kokubo, T. Nakamura, J. Biomed. Mater. Res. 54 (2001) 198.
[4] P. Tengvall, H. Elwing, I. Lundstrom, J. Colloid Interface Sci. 130 (1989) 405.
[5] P. Tengvall, H. Elwing, L. Sjoqvist, I. Lundstrom, L.M. Bjursten, Biomaterials 10 (1989) 118.
[6] P. Tengvall, I. Lundstrom, L. Sjoqvist, H. Elwing, Biomaterials 10 (1989) 166.
[7] J.M. Wu, S. Hayakawa, K. Tsuru, A. Osaka, Scr. Mater. 46 (2002) 705.
[8] X.X. Wang, S. Hayakawa, K. Tsuru, A. Osaka, J. Biomed. Mater. Res. 52 (2000) 171.
[9] J.M. Wu, J. Cryst. Growth 269 (2004) 347.
[10] J.M. Wu, T.W. Zhang, Y.W. Zeng, S. Hayakawa, K. Tsuru, A. Osaka, Langmuir 21 (2005) 6995.
[11] X.X. Wang, S. Hayakawa, K. Tsuru, A. Osaka, Biomaterials 23 (2002) 1353.
[12] V.S. Zhernakov, V.V. Latysh, V.V. Stolyarov, A.I. Zharikov, R.Z. Valiev, Scr. Mater. 44 (2001) 1771.
[13] V.V. Stolyarov, Y.T. Zhu, T.C. Lowe, R.Z. Valiev, Mater. Sci. Eng., A 303 (2001) 82.
[14] K. Lu, J. Lu, J. Mater. Sci. Technol. 15 (1999) 193.
[15] K. Lu, J. Lu, Mater. Sci. Eng., A 375 (2004) 38.
[16] K.Y. Zhu, A. Vassel, F. Brisset, K. Lu, J. Lu, Acta Mater. 52 (2004) 4101.
[17] U. Balachandran, N.G. Eror, J. Solid State Chem. 42 (1982) 276.
[18] A. Osaka, K. Tsuru, S. Hayakawa, Phosphorus Res. Bull. 17 (2004) 130.
[19] P. Falaras, A. Hugot-Le Goff, M.C. Bernard, A. Xagas, Sol. Energy Mater. Sol. Cells 64 (2000) 167.
[20] C. Ooka, H. Yoshida, S. Takeuchi, M. Maekaw, Z. Yamada, T. Hattori, Catal. Letters 5 (2004) 49.
[21] W.P. Tong, N.R. Tao, Z.B. Wang, J. Lu, K. Lu, Science 299 (2003) 686.
[22] J.F. Gu, D.H. Bei, J.S. Pan, J. Lu, K. Lu, Mater. Lett. 55 (2002) 340.
[23] Z.B. Wang, N.R. Tao, W.P. Tong, J. Lu, K. Lu, Acta Mater. 51 (2003) 4319.
[24] Z.B. Wang, J. Lu, K. Lu, Acta Mater. 53 (2005) 2081.